

In Situ UV-cured Composite Electrolyte for Highly Efficient Quasi-Solid-State Lithium Ion Batteries with Wide Temperature Range Applications

Pengcheng Zhou,^{*a} Yuxian Liu,^b Jian Chen,^a Shouqiang Lu,^a and Huiyang Li^{*c}

^a Guangdong Shunde Innovative Design Institute, Foshan 528300, P. R. China.

^b School of Integrated Circuits, Peking University, Beijing, 100871 P. R. China.

^c College of Chemistry and Chemical Engineering, Zhongkai University of Agriculture and Engineering, Guangzhou 510275, P. R. China.

*Corresponding author. *E-mail addresses:* zhoupc12358@163.com (Pengcheng Zhou) and lihuiyang@whu.edu.cn (Huiyang Li).

Instruments and measurements

Thermo-gravimetric analysis (TGA) was performed on SHIMADZU DTG-60 AH thermal analyzer at a heating rate of $10\text{ }^{\circ}\text{C min}^{-1}$ under nitrogen atmosphere with a flow rate of $20\text{ cm}^3\text{ min}^{-1}$ from 40 to $800\text{ }^{\circ}\text{C}$. The differential scanning calorimeter (DSC) was conducted on SHIMADZU DSC-60 at a heating rate of $10\text{ }^{\circ}\text{C min}^{-1}$ in nitrogen from -80 to $120\text{ }^{\circ}\text{C}$. The morphology of the samples was tested by field-emission scanning electron microscopy (SEM, Nova NanoSEM450, FEI). Cross-sectional samples were obtained through liquid nitrogen quenching. Phase structures were determined via X-ray powder diffraction (XRD) using a Bruker D8 Advance diffractometer. The element concentration was measured by inductive coupled plasma (ICP) optical emission spectroscopy (OES) using a Varian 710-ES spectrometer. The cyclic voltammetry (CV) of LE was conducted on a CS310M electrochemical workstation at a scan rate of 1 mV s^{-1} from 0 to 3 V (vs. Li/Li⁺) at $25\text{ }^{\circ}\text{C}$, using a three-electrode cell, where a platinum plate was used as working electrode and Li foil was used as the counter and reference electrodes. The CV of IPCE-PEO-Li was studied using an SS/electrolyte/Li configuration and fabricated to a CR2032-type cell. The IPCE layer was in situ prepared on the stainless steel substrate using a similar fabrication process to that of the electrodes in the full batteries, and then assembled with lithium disc, where the diameter of the stainless steel and the lithium discs was 16 mm. Linear sweep voltammetry (LSV) curves of the electrolytes were measured using an SS/electrolyte/Li configuration cell with a scanning rate of 1 mV s^{-1} from 1 to 6 V (vs. Li/Li⁺) at $25\text{ }^{\circ}\text{C}$. The battery performance was tested by a Neware CT-4008Tn-5 V50 mA-164 battery testing system. Environmental temperature was controlled by MT3065 environmental equipment.

Lithium ionic conductivity (σ) was tested via electrochemical impedance spectroscopy (EIS) with a stainless steel (SS)/IPCE/stainless steel (SS) device structure at 288–338K. The device

fabrication process was similar to that for the electrodes in the full batteries. Firstly, the electrolyte slurries were coated onto the polished stainless steel substrate followed by exposure under UV light (10 W, $\lambda = 365$ nm) at a distance of 1 inch to create a uniformly IPCE layer. Subsequently, the device was fabricated with two prepared stainless steel discs coated by the IPCE and assembled using a Swagelok symmetric cell with two stainless-steel rods.¹ The frequency ranges from 10^{-2} to 10^6 Hz with an amplitude of 10 mV. And σ was calculated with the equation below.^{2, 3}

$$\sigma = L/(R \times S)$$

Where R, L, and S represent the bulk resistance, electrolyte thickness, and the area, respectively.

The activation energy (E_a) of the battery was calculated according to the Arrhenius equation:

$$\sigma = A \times \exp(-E_a/kT)$$

Where A refers to the pre-exponential factor, T represents the temperature, and σ is the ionic conductivity of the IPCE.

Li-ion transference number (t_{Li^+}) was measured by a DC polarization method and calculated as the following equation.⁴ The device fabrication process was similar to that for the electrodes in the full batteries. Firstly, the electrolyte slurries were coated onto the lithium foil with a diameter of 16 mm, followed by exposure under UV light (10 W, $\lambda = 365$ nm) at a distance of 1 inch to create a uniform IPCE layer. Subsequently, the device was fabricated with two prepared lithium discs coated by the IPCE and assembled to a 2032-type cell.

$$t_{Li^+} = I_{ss}(\Delta V - R_0 I_0) / I_0(\Delta V - R_{ss} I_{ss}).$$

where ΔV represents the polarization potential (10 mV), R_0 , I_0 and R_{ss} , I_{ss} are the passive layer

resistance and current at the beginning and steady-state.

Table S1. Characteristics of the NMC111 cathode and LTO anode.

	Thickness of the active materials (μm)	Areal Density (mg cm^{-2})	compact density (mg cm^{-3})	Content of the active materials
NMC111 cathode	55	13	2.36	90%
LTO anode	76	12.5	1.65	89%

The thickness of the Al collector is 20 μm .

Table S2. Discharge rate performance data of NMC111/ Electrolyte /LTO configuration cells with different electrolyte components

Batteries	0.1C	0.2C	0.5C	Cycling number
LE	119	108	80	98
NMC111/IPCE/LTO	110	60	12	122 ^a
NMC111/IPCE-PEO/LTO	134	111	75	22 ^b
NMC111/IPCE-PEO-S/LTO	40	11	-	-
NMC111/IPCE-PEO-0.2%Li/LTO	134	120	87	36 ^b
NMC111/IPCE-PEO-1%Li/LTO	136	128	96	154 ^b
NMC111/IPCE-PEO-3%Li/LTO	135	120	57	119 ^b
NMC111/IPCE-PEO-Li-10%LALZO/LTO	127	106	52	64 ^b
NMC111/IPCE-PEO-Li-30%LALZO/LTO	127	106	43	168 ^b

^aCycling test was conducted @0.1C with a current density of 0.13 mA cm^{-2} , and the testing was terminated when the specific capacity decayed below 80% of the initial value. ^bCycling test was conducted @ 0.2C with a current density of 0.3 mA cm^{-2} , and the testing was terminated when the specific capacity decayed below 80% of the initial value. The test temperature was controlled to be 25 °C. The unit of the specific capacities is mAh g^{-1} .

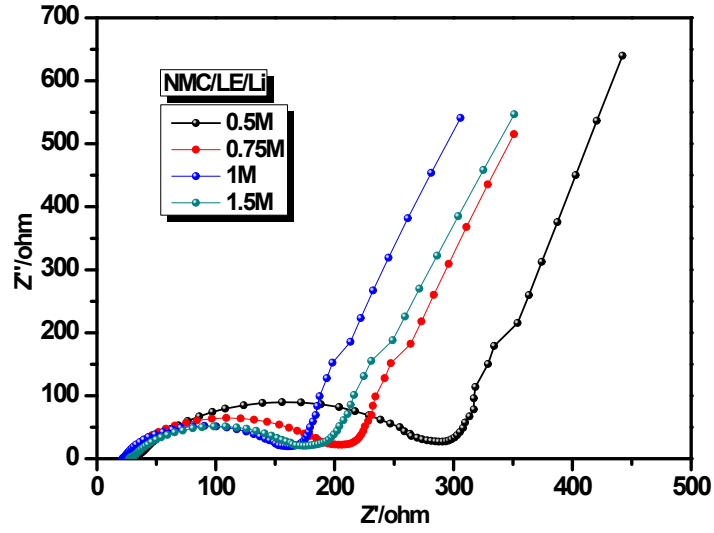


Figure S1. Ac impedance spectra of NMC111/SBN-based liquid electrolyte (LE)/Li cells with different concentrations.

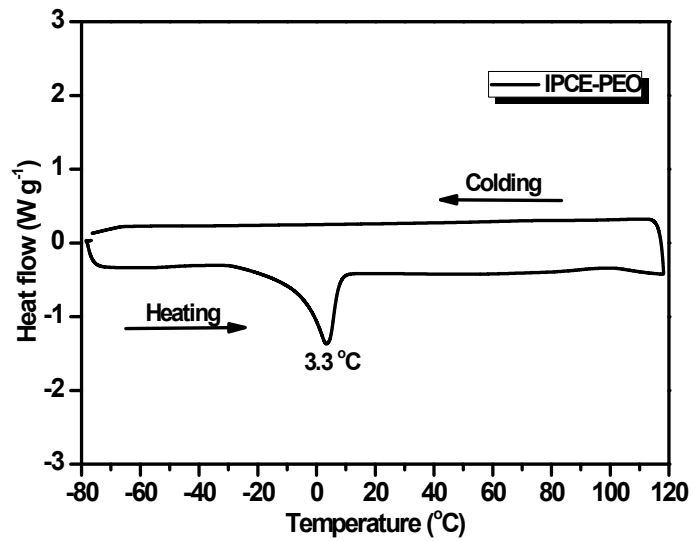


Figure S2. DSC profile of the IPCE-PEO composite electrolyte.

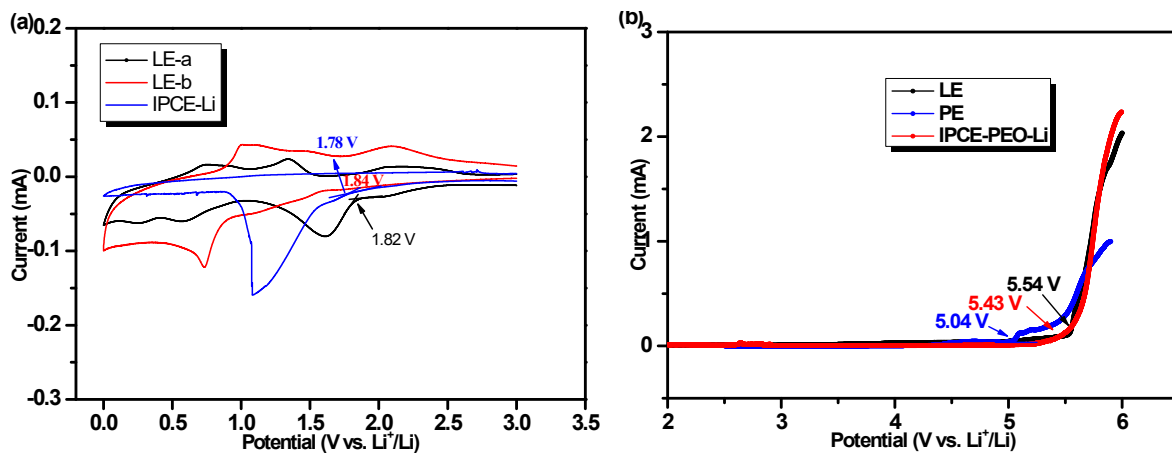


Figure S3. Cyclic voltammogram curves of LiTFSI-SBN liquid electrolyte (LE) tested in a three-electrode cell (LE-a), LE tested in a SS/LE/Li cell and the composite electrolyte (IPCE-PEO-Li) using an SS/electrolyte/Li cell with a scanning rate of 1 mV s^{-1} from 0 to 3 V (vs. Li/Li^+) at $25 \text{ }^\circ\text{C}$ (a). LSV curves of LiTFSI-SBN liquid electrolyte (LE), polymer electrolyte with LiTFSI-SBN (PE) and the composite electrolyte (IPCE-PEO-Li) using an SS/electrolyte/Li configuration cell with a scanning rate of 1 mV s^{-1} from 2 to 6 V (vs. Li/Li^+) (b).



Figure S4. The picture of a Swagelok symmetric cell with two stainless-steel rods.

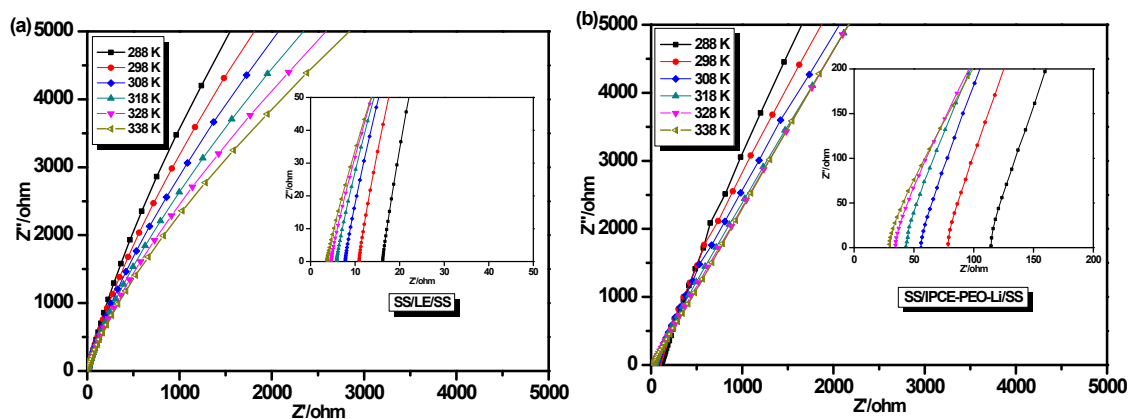


Figure S5. Electrochemical impedance spectroscopy of LE (a) and IPCE-PEO-Li (b) using a stainless steel (SS)/electrolyte/SS device structure, within the temperature range from 15 to 65 °C. Inset shows the high-magnification view of the EIS. The thickness of the IPCE-PEO-Li membrane was measured to be 200 μm , while the polypropylene (PP) separator used in the LE cell was 16 μm .

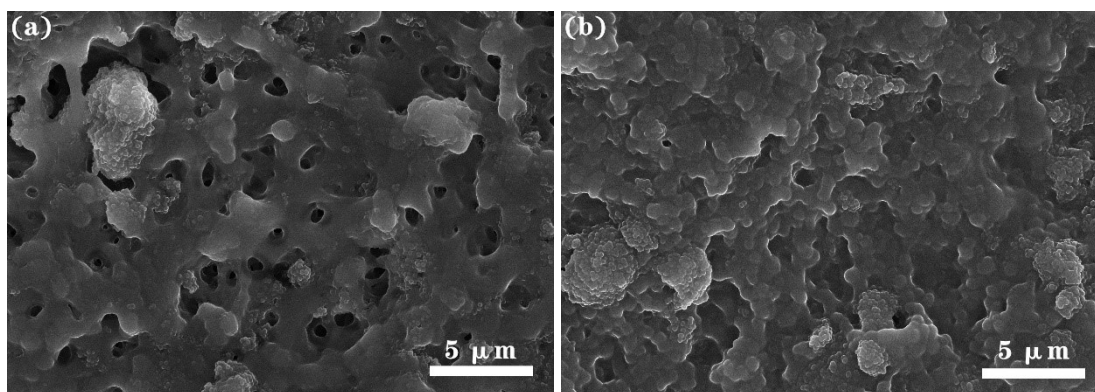


Figure S6. Surface SEM images of the PE coated NMC111 cathode (a) and LTO anode (b).

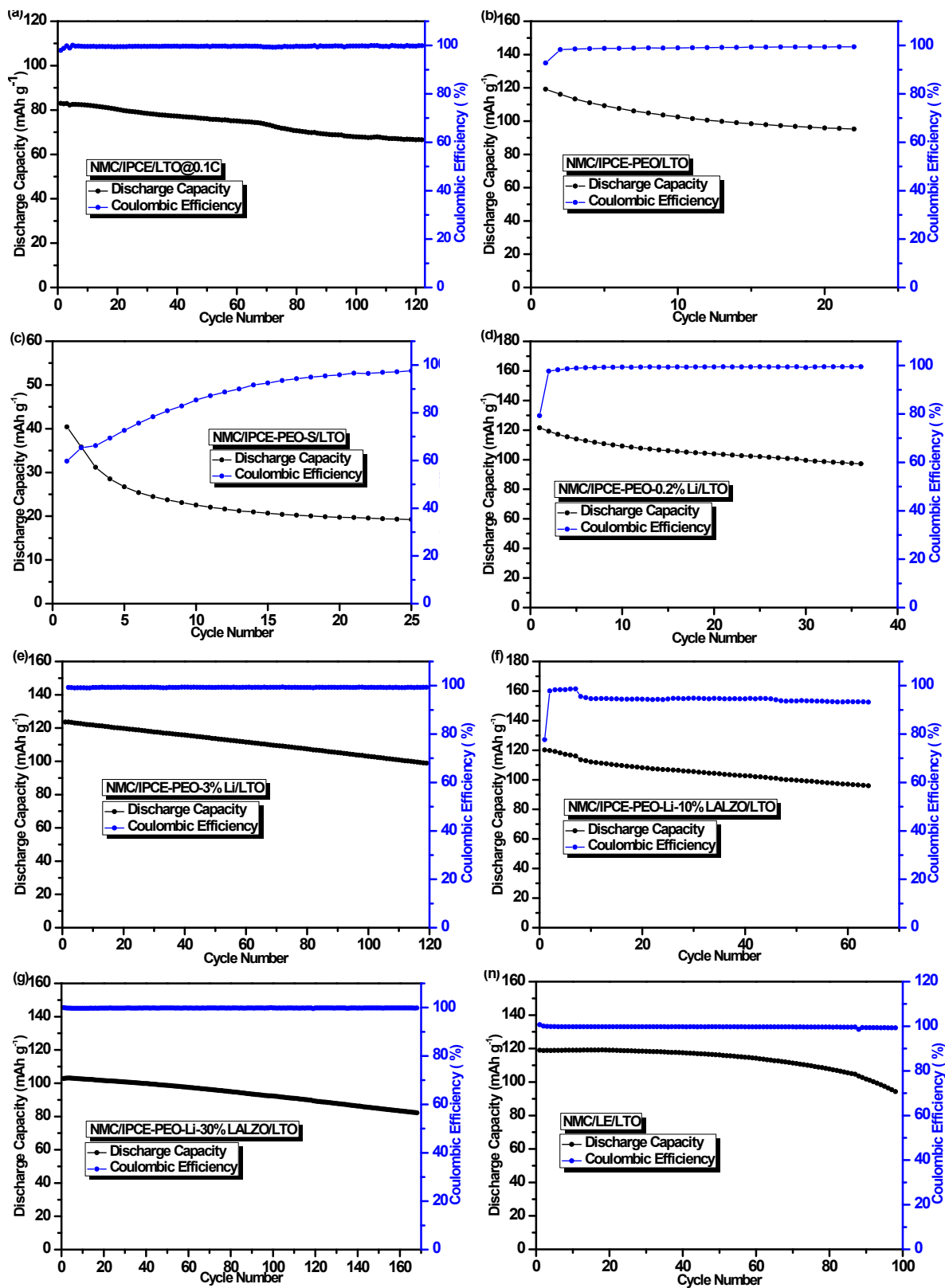


Figure S7. Discharge cycling performances of the NMC111/IPCE/LTO (a), NMC111/IPCE-PEO/LTO (b), NMC111/IPCE-PEO-S/LTO (c), NMC111/IPCE-PEO-0.2%Li/LTO (d),

NMC111/IPCE-PEO-3%Li/LTO (e), NMC111/IPCE-PEO-Li-10%LALZO/LTO (f),
 NMC111/IPCE-PEO-Li-30%LALZO/LTO (g), NMC111/LE/LTO (h) cells tested at 25 °C.

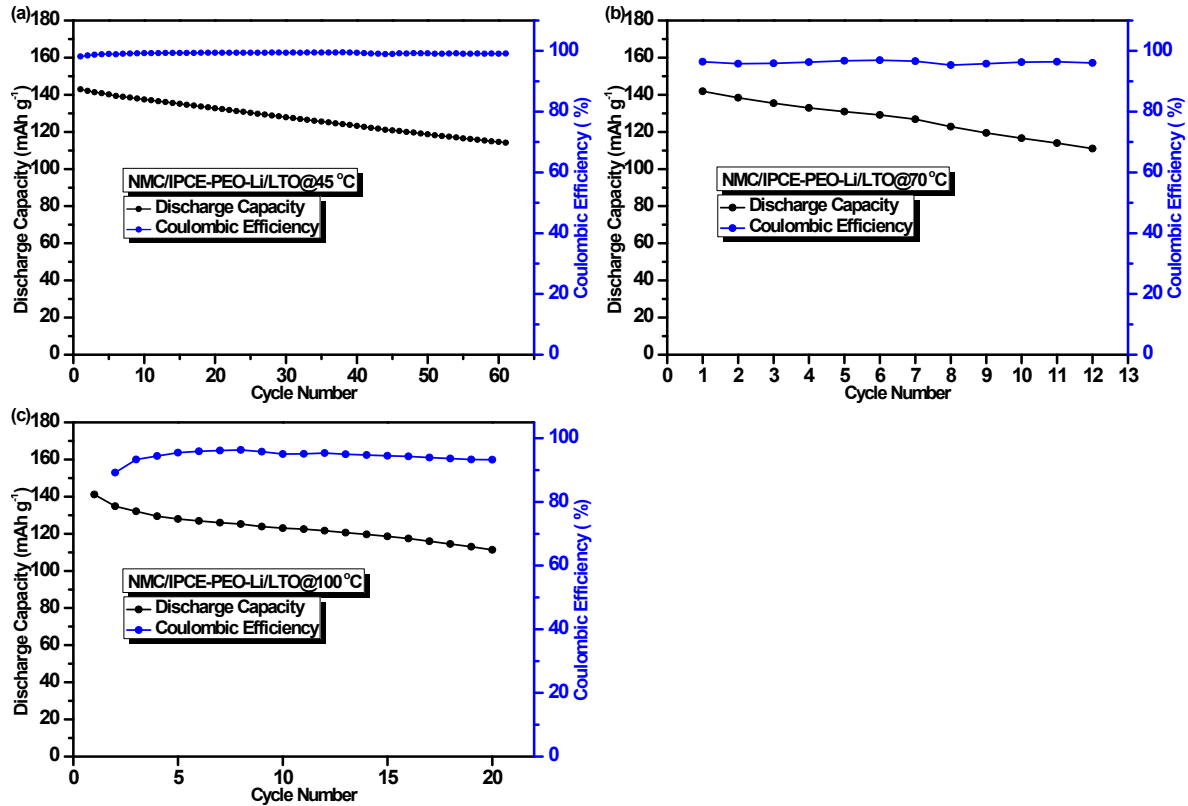


Figure S8. Discharge cycling performances of the NMC111/IPCE-PEO-Li-LALZO/LTO cells at 45 (a), 70 (b) and 100 °C (c).

Table S3. Charge/discharge diagrams at different temperatures

Temperature	Charge Capacity (mAh g ⁻¹)	Discharge Capacity (mAh g ⁻¹)	Cycling number ^a
25 °C	135	128	154
45 °C	145	143	60
70 °C	147	142	12
100 °C	144	141	21

^a The discharge cycling performances were tested at 0.2C with a current density of 0.3 mA cm⁻² and terminated when the specific capacity decayed below 80% of the initial performance.

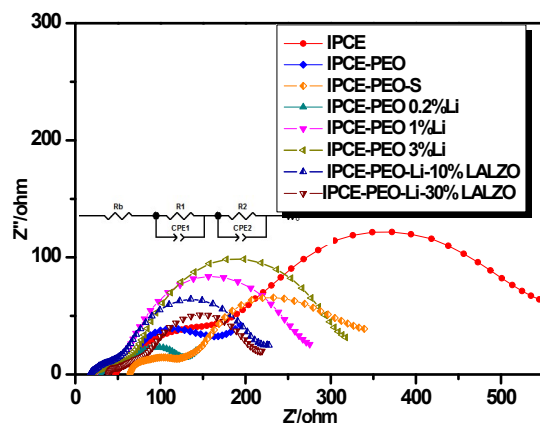


Figure S9. Ac impedance spectra of NMC111/Electrolyte/LTO configuration cells with various electrolyte components after cycling at 25 °C, the inset shows the equivalent circuit of the cells.

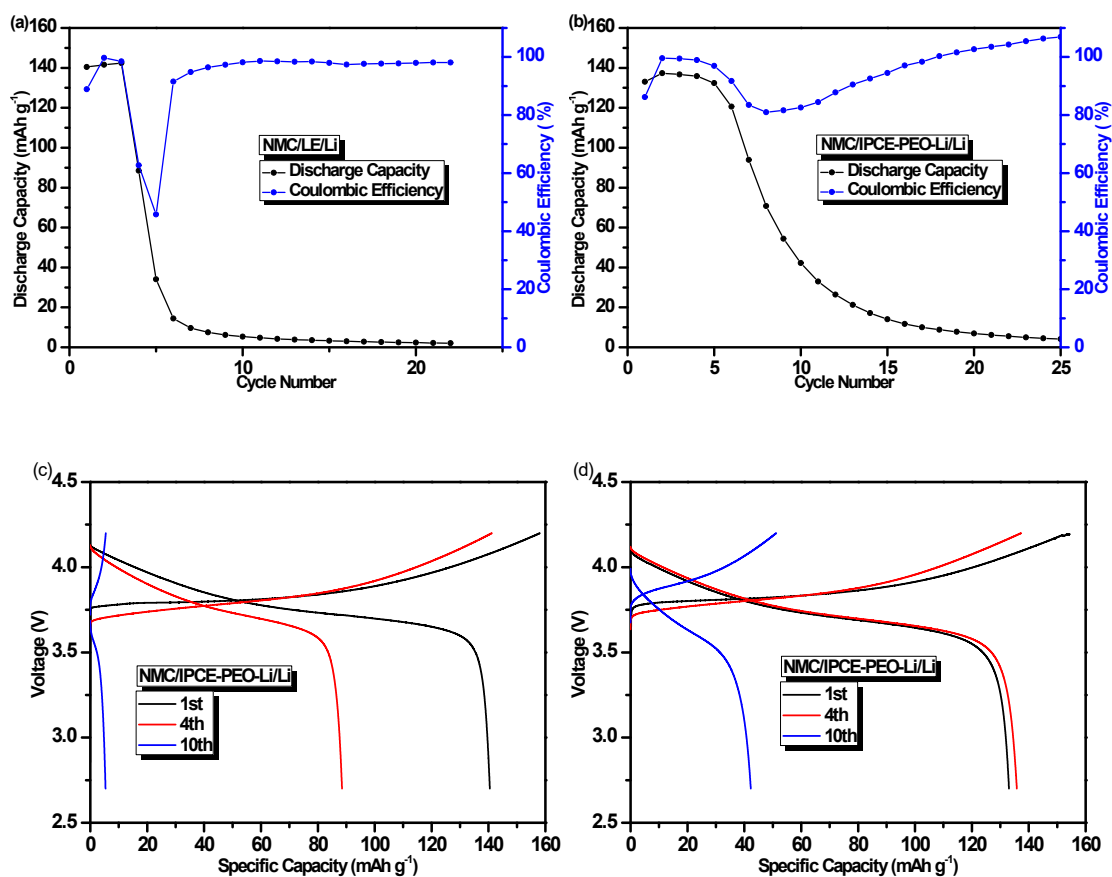


Figure S10. Discharge cycling performances of the NMC111/LE/Li (a), (c) and NMC111/IPCE-PEO-Li/Li (b), (d) cells between 2.7 and 4.2 V at 25 °C, wherein the current density is 0.15 mA cm⁻² (0.1C).

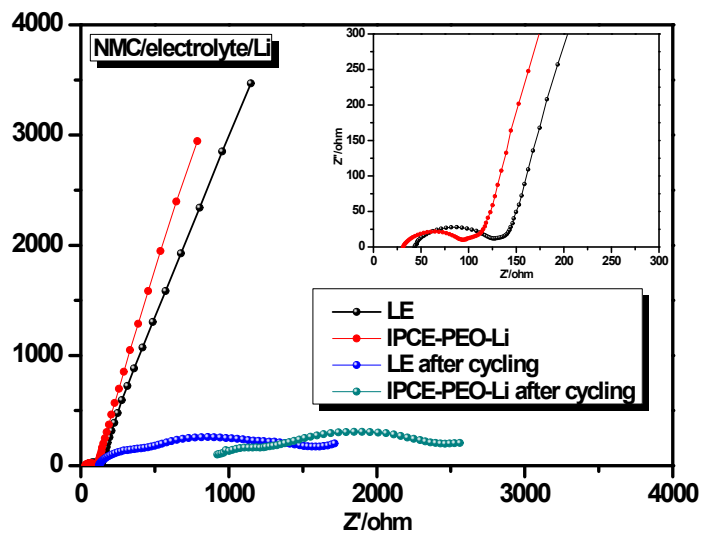


Figure S11. AC impedance spectra of NMC111/LE/Li and NMC111/ IPCE-PEO-Li /Li cells before and after cycling. Inset shows the high-magnification view of the EIS.

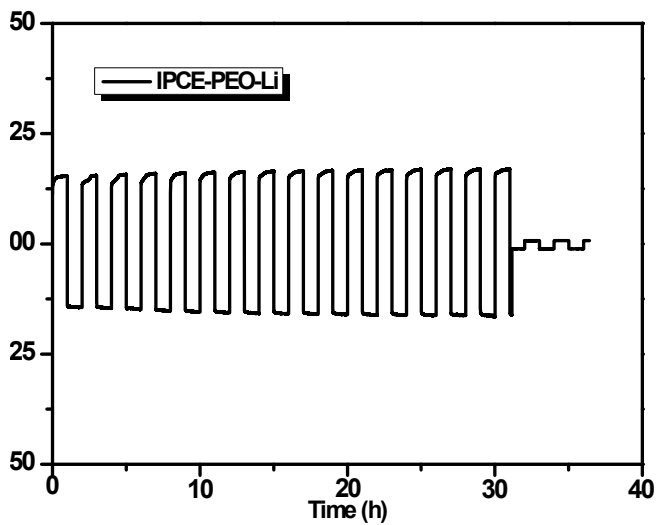


Figure S12. Li plating/stripping performance of the Li/IPCE-PEO-Li/Li symmetric cell at a current density of $0.1 \text{ mA cm}^{-2}/0.1 \text{ mAh cm}^{-2}$ at $25 \text{ }^\circ\text{C}$.

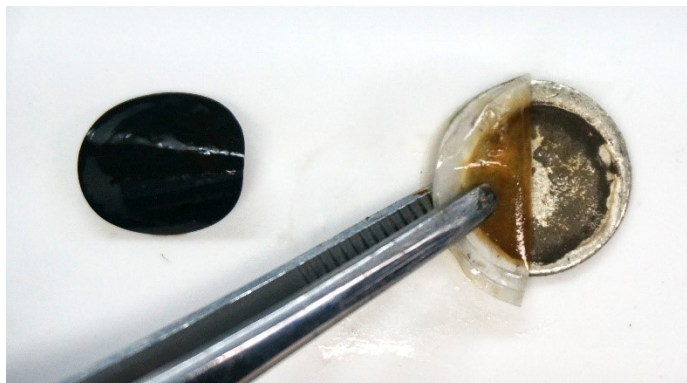


Figure S13. The picture of the electrodes inside the cycled NMC111/LE/Li cell after disassembling in the Argon-filled glovebox.

References

- (1) X. Yu, Y. Liu, J. B. Goodenough and A. Manthiram, *ACS Appl. Mater. Interfaces*, 2021, 13, 30703-3071.
- (2) I. Shin, J. Nam, K. Lee, E. Kim and T.-H. Kim, *Polym. Chem.*, 2018, 9, 5190-5199.
- (3) C. Zuo, H. Li, G. Chen, J. Yang, Z. Xu and Z. Xue, *ACS Appl. Energy Mater.*, 2021, 4, 9402-9411.
- (4) K. Borzutzki, J. Thienenkamp, M. Diehl, M. Winter and G. Brunklaus, *J. Mater. Chem. A*, 2019, 7, 188-201.